The Thermal Decomposition of Mg – Al Hydrotalcites: Effects of Interlayer Anions and Characteristics of the Final Structure

Jules C. A. A. Roelofs, Jeroen A. van Bokhoven, A. Jos van Dillen, John W. Geus, and Krijn P. de Jong*[a]

Abstract: The thermal decomposition of hydrotalcites (HTs) with different interlayer anions in the 298 – 523 K region has been investigated by using transmission electron microscopy (TEM), thermogravimetric analysis (TGA), X-ray diffraction (XRD), and IR, ^{27}Al MAS-NMR and X-ray absorption near-edge structure (XANES) spectroscopy. The thermal stability of the HT with interlayer oxalate was remarkably higher than that of HTs with interlayer carbonate; the onset temperatures for decomposition were 523 K and 473 K, respectively. It is proposed that the basicity of the interlayer anion is the key factor in the onset of dehydroxylation of the brucite-like layers: the lower the basicity, the more thermally stable the HT compound. After heat treatment at 723 K, small Mg(Al)O domains ($\approx$5 nm) within the HT crystallites cause broadening of the XRD reflections. The electron diffraction pattern consists of spots and rings, due to non-randomly oriented crystalline material. Formation of disordered bonds, caused by nonideal packing between the decomposing adjacent cation layers in the (1 1 1) direction, could explain the expanded *d* value in the resulting MgO-like phase observed with XRD and electron diffraction. The orientation of the Mg(Al)O domains in the heat-treated material may be crucial for the so-called "memory effect" of HTs.

Keywords: basicity · decomposition · hydrotalcites · layered compounds · oxalate

Introduction

Hydrotalcite (HT) has attracted much attention during the development of new environmentally friendly catalysts. After calcination at up to 725 – 775 K, HT decomposes to a mixed oxide of high surface area, with strong Lewis base features.[1] Consequently, calcined HTs are suitable catalysts for several vapour-phase base-catalyzed condensation reactions.[2–6] When heat-treated HTs are brought into contact with water at room temperature, restoration of the layered structure with mainly OH^- ions in the interlayer proceeds,[7] yielding a highly active base catalyst suitable for liquid-phase aldol condensation reactions.[8–12] The structure and activity of the HT-like compounds thus produced depend to a large extent on the treatment applied. Therefore, insight into the changes in the HT during activation is vital, as well as knowledge of the structure resulting after heat treatment.

The structure of HT, $Mg_6Al_2(OH)_{16}CO_3 \cdot 4H_2O$, resembles that of brucite, $Mg(OH)_2$. In the latter the magnesium cations are octahedrally coordinated by hydroxyl ions, resulting in stacks of edge-shared layers of octahedra. In the HT structure, some of the Mg^{2+} ions are replaced by Al^{3+} ions, resulting in positively charged layers whereby the charge is compensated by interlayer anions, in this case carbonate. Furthermore, water molecules are present in the interlayer.[13–15]

Physisorbed and interstitial water is removed from HT at temperatures above $\approx$373 K and $\approx$460 K, respectively. At more elevated temperatures (above 523 K) the HT undergoes dehydroxylation and decarboxylation with H_2O and CO_2 evolution, giving rise to a material of increased surface area and formation of micropores.[13] During the thermal treatment the coordination of Al is partly lowered from octahedral to tetrahedral, as can be concluded from ^{27}Al MAS-NMR measurements;[16–19] this is indicative of the start of the cation layer dehydroxylation.

The onset and the origin of the Mg – Al HT decomposition are still subjects of discussion. Several studies have been undertaken to elucidate the observed changes, especially in the low-temperature region up to 573 K. Kanezaki suggested that the reaction of carbonate anions and interlayer water yields gaseous carbon dioxide and charge-compensating hydroxyl anions within the interlayer.[26] Others postulate the reaction of hydroxyl groups from the cation layer with interlayer carbonate.[20] Although these explanations differ, both approaches take the line that the decomposition depends

[a] Dr. J. C. A. A. Roelofs, Prof. K. P. de Jong, Dr. J. A. van Bokhoven, Dr. A. J. van Dillen, Prof. J. W. Geus
Department of Inorganic Chemistry and Catalysis
Debye Institute, Utrecht University, Postbus 80083
3508 TB Utrecht (The Netherlands)
Fax: (+31) 30-2511027
E-mail: k.p.dejong@chem.uu.nl

  0947-6539/02/0824-5571 $ 20.00+.50/0

on the nature of the interlayer anion. However, the influence of interlayer anions other than carbonate on the thermal decomposition of Mg–Al HT has not been investigated fully. Recently, Xu and Peng reported that Mg–Al HTs with interlayer nitrate show remarkable thermal stability of the layered structure.[21]

As mentioned, thermal treatment at up to 723–773 K results in the formation of a mixed oxide. Most of the broad X-ray diffraction (XRD) reflections of this heat-treated HT can be attributed to an MgO-like phase, which arises above 573 K. Besides (or as a part of) this, reflections due to a spinel-type compound are present. The exact nature of the MgO-like phase is not clear, since it is very difficult to distinguish between small nuclei of $MgAl_2O_4$, Al_2O_3 or Al-doped MgO.[22–24] MacKenzie stated that the broadening of the XRD reflections of the MgO-like phase is due to poor crystallinity or small particle size, or to both.[17] The lattice constant *a* of decomposed HT is smaller than that of pure MgO and decreases at temperatures up to 673 K; this indicates that Al^{3+} ions, which have a smaller ionic radius than Mg^{2+} ions, enter into MgO. Above 1073 K, *a* increases rapidly towards the value for pure MgO because of Al^{3+} ion migration, and $MgAl_2O_4$ formation has been observed at 1173–1273 K.[7, 25, 26] Repeated calcination–rehydration cycles result in the segregation of Al^{3+} from the cation layer and in the formation of spinel nuclei.[27] Bright-field transmission electron microscopy (TEM) images of calcined HTs show that the sizes of the original platelets present after synthesis are retained upon thermal treatment.[28–30]

We showed previously with in situ XANES (X-ray absorption near-edge structure) at the Mg and Al K-edges that Mg^{2+} and Al^{3+} in the cation layers of HTs with interlayer carbonate behave differently according to the temperature.[31] At 425 K the coordination of some octahedral Al is already lowered, whereas the Mg coordination does not show any modification. Most remarkable is that HT treated at 425 K and measured at room temperature shows a return to the original octahedral Al coordination. It has been proposed that an Al–OH bond breakage occurs at about 425 K, without removal of H_2O. This bond is restored at room temperature.

It is interesting to examine whether the observed features in Mg–Al HT also depend on the nature of the interlayer anion. Since the HT structure has many structural parameters (for example, the nature of the di- and trivalent cations as well as their ratio), assignment of key factors influencing the decomposition often has ambiguous results. We therefore studied the decomposition in the range from room temperature to 523 K of two very similar Mg–Al HTs with chemically much alike anions, carbonate and oxalate (HT-CO_3 and HT_{ox}), using techniques covering the important parameters: that is, the coordination of Mg^{2+} and Al^{3+} (in situ XANES and ^{27}Al MAS-NMR spectroscopy), changes in crystallinity and interlayer spacing (XRD), the weight loss and nature of evolved gases [thermogravimetric analysis mass spectrometry (TGA-MS)], and in situ changes in IR vibrations. Unique in situ measurements at the Mg and Al K-edges at these elevated temperatures show the great potential of the XANES technique. We have detected large differences in thermal behaviour of the two HT compounds, which can now be ascribed solely to the nature of the interlayer anion. We also studied the structure of the heat-treated HTs. For the first time, both bright- and dark-field TEM as well as electron and X-ray diffraction were used; this gave greater insight into the nature and crystallinity of the resulting MgO-like phase after heat treatment.

Results and Discussion

Influence of interlayer anion on the dehydroxylation of Mg–Al hydrotalcites: In general, TGA results of HT compounds reveal two distinct weight losses, of which the first is ascribed to removal of interlayer water up to 453–473 K and the second to dehydroxylation and decarboxylation above 573 K.[13] The TGA-MS results of the HT-CO_3 confirm this behaviour (Figure 1a). It is striking that the amount of

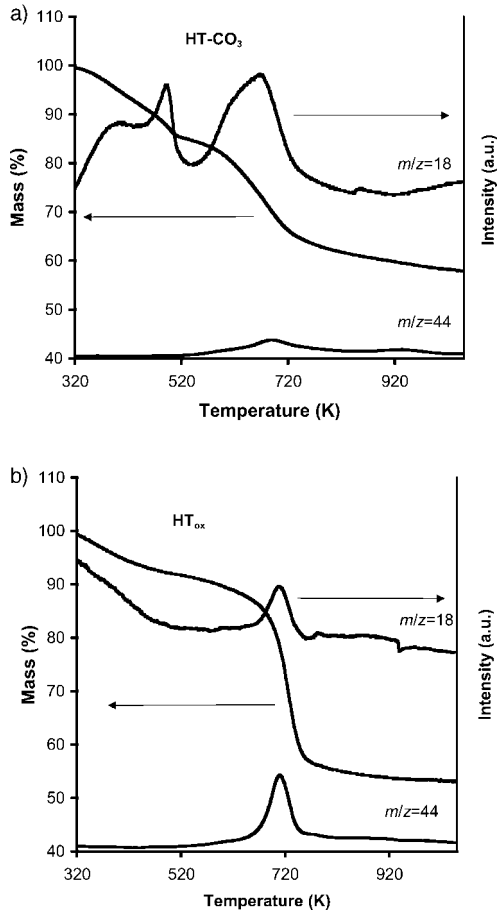

Figure 1. TGA-MS of a) HT-CO_3, b) HT_{ox}; $m/z = 18$ (H_2O), $m/z = 44$ (CO_2).

interlayer water in HT_{ox} is relatively small, resulting in a low weight loss (8%) up to 523 K (Figure 1b), relative to the HT-CO_3, which loses about 15% of its weight. Above this temperature the cation layers start to decompose, resulting in the observed evolution of water with a maximum at 673 K for HT-CO_3 and 710 K for HT_{ox}. We attribute the CO_2 evolution from the HT_{ox} above 710 K to decomposition of interlayer

  0947-6539/02/0824-5572 $ 20.00+.50/0 *Chem. Eur. J.* **2002**, *8*, No. 24

oxalate, which is also accompanied by simultaneous dehydroxylation of the cation layer.

The ex situ XRD pattern of the HT-CO_3 at room temperature shows the characteristics of a highly crystalline layered structure (Figure 2a).[13] We calculated the basal interlayer spacing from the strong symmetric (003) reflection ($2\Theta = 13.4^\circ$). If the thickness of the brucite-like layer is assumed

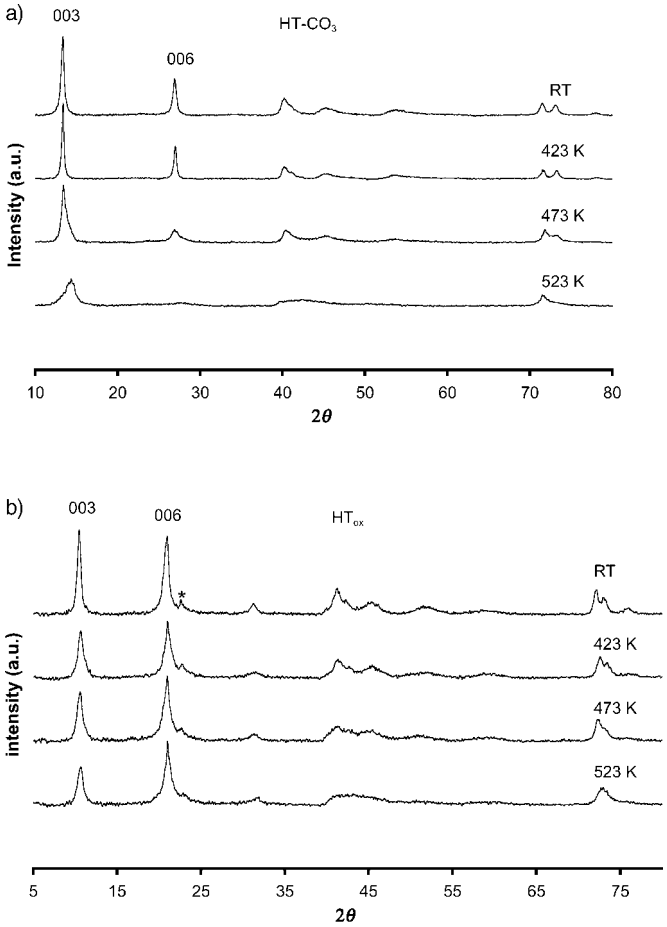

Figure 2. Ex situ XRD patterns of a) HT-CO_3 and b) HT_{ox} preheated at the temperatures indicated.

to be 4.8 Å,[32] the interlayer distance corresponds to 2.9 Å. The presence of oxalate in the interlayer gives rise to a (003) reflection at 9.8 Å ($2\Theta = 10.6^\circ$) and thus an interlayer distance of 5.0 Å, which is in close agreement with values reported in the literature.[57, 33] The reflection at 4.6 Å ($2\Theta = 22.7^\circ$) marked by an asterisk in the HT_{ox} pattern (Figure 2b) can be assigned to a superlattice in the *ab* plane of the HT, indicating a high degree of cation ordering, probably induced by the high fraction of Al and the strong interactions between the interlayer oxalate and the cation layer. Vucelic et al. reported the same reflection in an HT (Mg/Al = 2) with interlayer benzoate.[34] Gastuche et al.[35] and Serna et al.[36] made similar observations. The ex situ XRD patterns of HT_{ox} did not show a significant decrease of the interlayer distance at 473 K (Figure 2b). After heating at 523 K, the *d* value of the (003) reflection of the HT-CO_3 had decreased from 7.7 Å to 7.1 Å and peak broadening occurred (Figure 2a). Another important change in the HT-CO_3 was the almost complete disappearance of the (006) reflection; this could result from distortion of the layered structure.[37] Surprisingly, the (003) reflection of the HT_{ox} did not shift to lower 2Θ values, even at 523 K (Figure 2b). High-temperature in situ XRD measurements revealed a significant shift of the (003) reflection of HT-CO_3 at 473 K.[26, 37, 38] Ex situ results with these compounds can differ substantially from in situ results; as described previously, in situ and ex situ XANES results at these temperatures differ.[31] Furthermore, the process of rehydration and reconstruction of HT upon exposure to air is very fast and reversible,[38] and thus affects the ex situ results. Indeed, when the X-ray diffraction pattern of an HT-CO_3 sample was measured in situ at high temperatures, a shift of the (003) diffraction maximum from $2\Theta = 13.7^\circ$ to 15.5° was observed at 473 K (Figure 3). In the in situ XRD pattern of HT_{ox}, on the

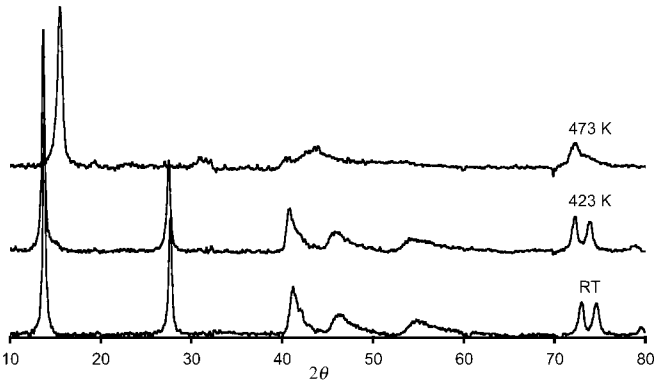

Figure 3. In situ XRD patterns of HT-CO_3 measured at the temperatures indicated.

other hand, no changes were evident in the (006) reflection at 523 K (data not shown); this demonstrates the thermal stability of HT_{ox}. Mg – Al HT compounds with chloride[38] and nitrate[21] as the compensating anion display a similar thermal stability. Grafting of anions in the brucite-like layer of HT-like compounds has been reported for a large variety of interlayer species. Malherbe and Besse showed an increased thermal stability in Mg – Al HTs with several oxo anions as a result of the grafting process.[39]

In general, an octahedral Al compound shows two resonances above the absorption edge, at 1568 and 1572 eV, whereas a tetrahedral compound shows a single sharp rising edge at 1566 eV. Moreover, the near edge (0 – 15 eV above the edge) in the spectrum of an octahedral compound has higher intensity than the near edge of a tetrahedral compound. Changes are seen to occur as a function of temperature during heating of the HT-CO_3 (Figure 4a). A gradual increase in the number of tetrahedral Al ions is evident from the intensity increase just on the absorption edge (indicated by an arrow). Furthermore, the decrease in the octahedral signal at 1572 eV is consistent with previous results.[31] Again, the HT_{ox} results (Figure 4b) differ from those obtained with HT-CO_3. According to XANES, no clear coordination changes of Al in HT_{ox} take place in the temperature region up to 473 K, whereas at

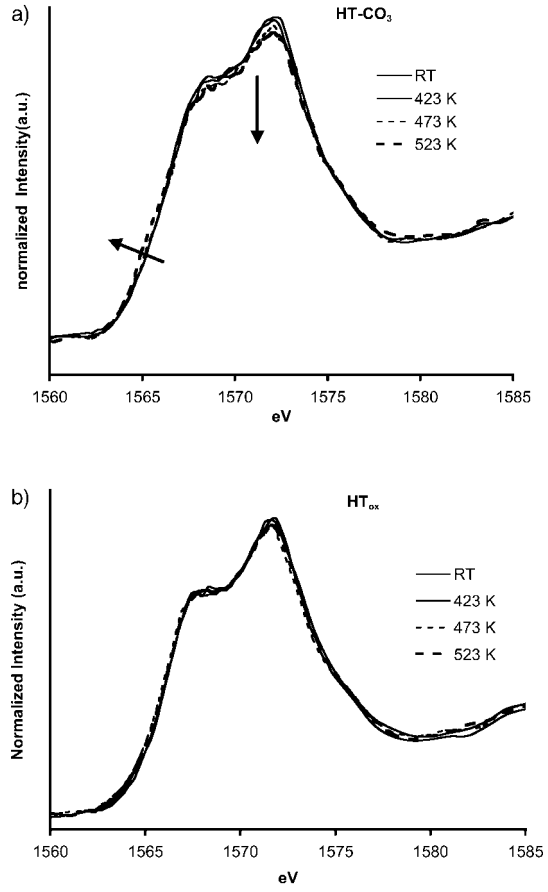

Figure 4. In situ Al K-edge XANES of a) HT-CO_3 and b) HT_{ox} measured at the temperatures indicated.

523 K only a minor proportion of the Al ions are tetrahedrally coordinated.

Changes in the Al coordination in the HT compounds were also studied with ^{27}Al MAS-NMR spectroscopy (Figure 5). The use of high spinning speeds (up to 30 kHz) and a high external magnetic field strength (14.1 T) minimizes the chance that some of the Al ions escape detection.[40] At room temperature, the NMR spectrum of HT-CO_3 shows a relatively narrow resonance peak at a chemical shift δ of 11.1, corresponding to octahedrally coordinated Al. Signals related to tetrahedral Al are usually found in the $\delta = 80-50$ region; the signals can be broadened and shifted because of the quadrupolar interaction of ^{27}Al.[41] Less than 1% of tetrahedral Al was present in the HT-CO_3 at room temperature (Table 1). The tetrahedral Al content gradually increased to 26% at 523 K after treatment. This can be concluded from the appearance of the broad resonance around $\delta = 80$. The HT_{ox} sample showed a single resonance at $\delta = 12.9$, that is, a slightly higher shift than was found with the HT-CO_3. This could be caused by the stronger influence of the oxalate anion on the Al ions in the cation layer. Although the percentage of tetrahedral Al^{3+} increased during heat treatment from room temperature to 523 K, it remained much lower than that observed with HT-CO_3. After heating of HT_{ox} to 523 K, around 10% of the Al^{3+} ions were found to be in tetrahedral coordination.

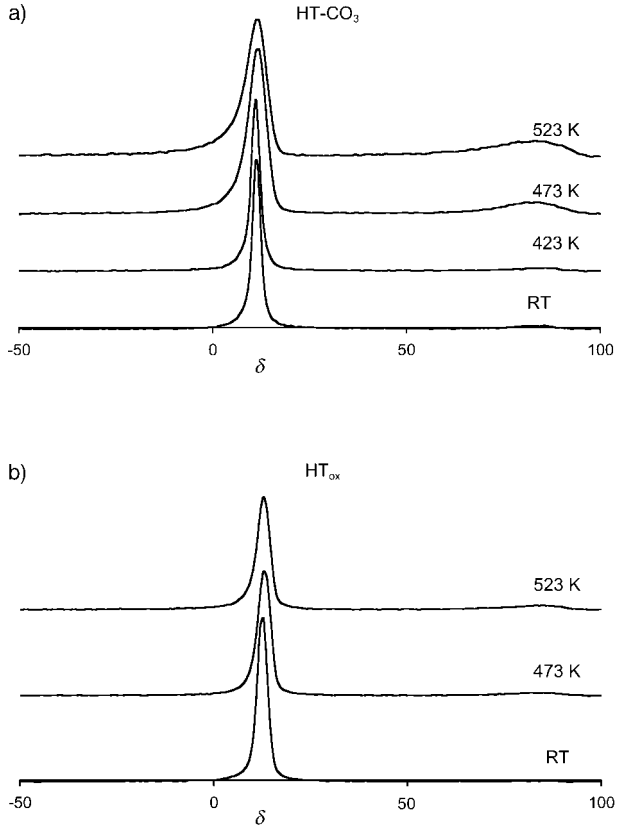

Figure 5. ^{27}Al MAS-NMR obtained at room temperature of a) HT-CO_3 and b) HT_{ox} preheated at the temperatures indicated.

Table 1. Tetrahedral Al percentages at room temperature and after heat treatment at 423 K, 473 K and 523 K according to ^{27}Al-MAS-NMR.

	RT	423 K	473 K	523 K
HT-CO_3	< 1	< 1	16	26
HT_{ox}	0	n.d.[a]	6	10

[a] n.d.: not determined.

The Mg K-edge spectra of the HT samples were obtained in situ at room temperature and 523 K (Figure 6). For the first time, changes in coordination of Mg have been measured in

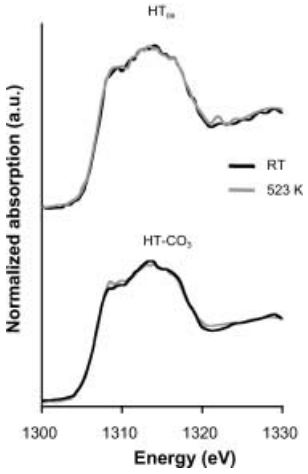

Figure 6. In situ Mg K-edge of HT_{ox} (top) and HT-CO_3 (bottom) measured at the temperatures indicated.

0947-6539/02/0824-5574 $ 20.00+.50/0 *Chem. Eur. J.* **2002**, *8*, No. 24

situ at this high temperature. The changes in the HT-CO_3 spectra from room temperature to 523 K are very similar to those observed during brucite dehydroxylation, which was studied by Yoshida et al. using ex situ Mg K-edge XANES.[42] Heating of HT-CO_3 to 523 K resulted in an intensity increase at 1310 eV. MacKenzie et al. reported changes at 473 K in the ^{25}Mg MAS-NMR of HT-CO_3. The authors ascribed the effect on the spectra to changes in coordination of neighbouring Al, rather than to the onset of the dehydroxylation of $Mg(OH)_6$ octahedra.[17] The spectra of HT_{ox} at room temperature and 523 K did not differ much at 1310 eV, being within the signal-to-noise ratio. As with Al K-edge XANES results, Mg^{2+} ions in HT_{ox} are much less sensitive to temperature than in HT-CO_3.

Peaks in the infrared spectra of HT-CO_3 and HT_{ox} recorded at room temperature, 423 K, 473 K and 523 K (Figure 7) have been assigned according to results reported in the literature.[13, 43–45] The hydroxyl stretching region consists of a broad

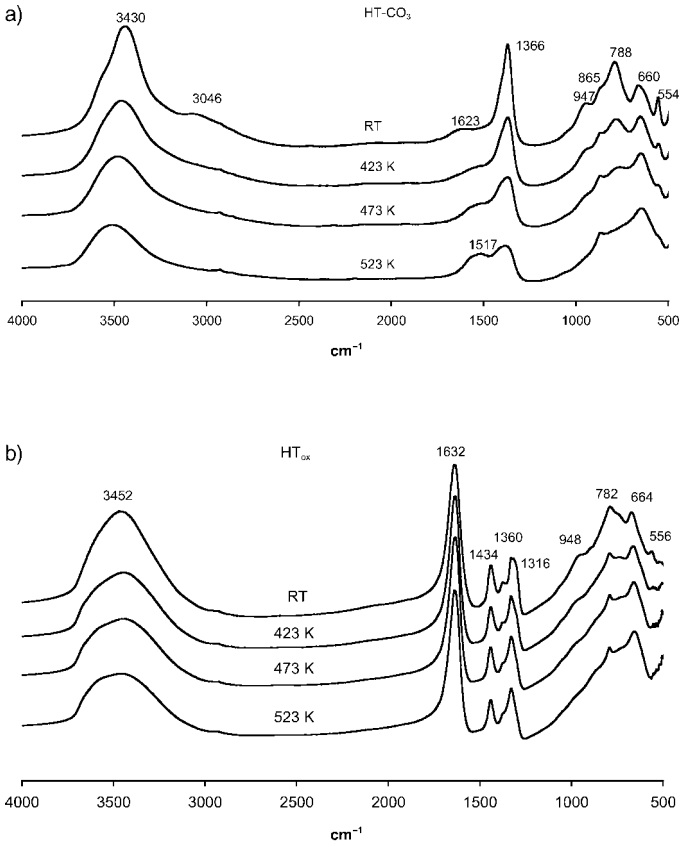

Figure 7. IR spectra of a) HT-CO_3 and b) HT_{ox} measured at the temperatures indicated.

antisymmetric peak around 3430 cm^{-1}, ascribed to the stretching mode of hydroxyls attached to Al and Mg. The shoulder at 3046 cm^{-1} recorded at room temperature is due to hydrogen bonding of interlayer water and interlayer carbonate. The bending mode of interlayer water is found at 1623 cm^{-1}. Several absorption bands can be assigned to interlayer carbonate: the antisymmetric υ_3 mode at 1366 cm^{-1}, the υ_2 mode at 865 cm^{-1} and the υ_4 mode at 660 cm^{-1}. The υ_4 mode coincides with the cation layer Mg–O stretching frequency. The bands at 554, 788 and 947 cm^{-1} can be attributed to Al–O stretching modes. Upon heating, removal of interlayer water had already occurred at 423 – 473 K, as can be concluded from the disappearance of both the broad shoulder at 3046 cm^{-1} and the signal at 1623 cm^{-1}. Raising the temperature to 423 K resulted in a decrease of the Al-related vibrations of the HT-CO_3 at 554, 788 and 947 cm^{-1}. Combined with the observed decrease in the absorption in the hydroxyl-stretching region at 3400 – 3600 cm^{-1}, this indicates the start of layer dehydroxylation. Changes in carbonate vibrations were also observed. A decrease in intensity of the υ_3 mode at 1366 cm^{-1} was accompanied by the appearance of a new signal at 1517 cm^{-1}, which was clearly visible in the pattern recorded at 523 K. This was accompanied by a slight increase in intensity around 1030 – 1050 cm^{-1}, which points to a rearrangement of the carbonate in the interlayer space. This band around 1030 – 1050 cm^{-1} is usually ascribed to the symmetrical stretching mode of carbonate. This vibrational mode is inactive when the carbonate ion retains its full symmetry.[25, 52, 56] Rey et al. ascribed these changes to alterations in carbonate symmetry from D_{3h} to C_{2v} or C_{3v}.[18] In our view, this could point to the formation of bicarbonate.

In general, interlayer anion absorption bands are found between 1200 and 1700 cm^{-1}.[13] No results concerning these bands in HT with interlayer oxalate are available in the literature. As the aim of our research has not been the complete elucidation of this IR spectrum, these bands for HT_{ox} (Figure 7) were not assigned in detail. Several of the interlayer anion bands are most probably associated with the (anti)symmetric stretch modes of the C=O moiety of the interlayer oxalate. The other bands observed can be assigned analogously to those of the HT-CO_3 and to results from the literature. More importantly, the interlayer absorption bands did not change much in intensity and position during heat treatment, in contrast to the IR results obtained with HT-CO_3. That dehydroxylation occurred in HT_{ox} can be concluded from the lowering of the Al-related signals at 556, 782 and 948 cm^{-1} and the decrease in the hydroxyl-stretching region, as we observed with HT-CO_3 also. From these results it is clear that interlayer oxalate stabilizes the HT layer at a higher temperature than carbonate.

In several HT-like compounds, for example, ZnAl and CuCr HTs containing (substituted) benzoates or sulfonates as interlayer anions,[46] grafting of the interlayer anion in the brucite-like layer has been reported as an explanation for the observed thermal stability. In the Mg – Al system also, several oxo anions show this tendency.[39] A strong indication for grafting is a decrease in the interlamellar distance such that the anion, based on its geometry, cannot fit into it (without cation layer dehydroxylation). On the basis of the observed changes in Al coordination (for the HT-CO_3) and the absence of a decrease in the (003) reflection for the HT_{ox}, other processes have to be taken into account. The presence of tetrahedrally coordinated Al at 473 K also excludes the model proposed by Stanimirova et al. for Mg – Al HT at 523 K.[47]

Below 473 K, some of the Al–O[H]–Mg bonds are broken. It is likely that a proton of a nearby OH group migrates to an OH attached to an Al^{3+}; this would weaken the Al–OH bond causing H_2O to form. At 473 K, this water remains strongly

  0947-6539/02/0824-5575 $ 20.00+.50/0

adsorbed on or even within the brucite-like layer and subsequent cooling to room temperature restores the original Al–O[H]–Mg bond.[31] Desorption of water originating from cation layer dehydroxylation from top layers of the HT crystallite could probably account for the 6% tetrahedrally coordinated Al in HT_{ox}, observed with ex situ ^{27}Al MAS-NMR spectroscopy at 473 K (Figure 5 and Table 1). Judging from the large amount of tetrahedrally coordinated Al in HT-CO_3 at 473 K, other processes have also to be taken into account, such as reaction of interlayer anions with cation hydroxyl groups, as mentioned for HT-CO_3.[17, 20] Figure 7 shows an IR intensity decrease for the Al-related vibrations in HT_{ox}, whereas the interlayer oxalate bands remained merely constant. In the case of HT-CO_3, besides the decrease in Al-related vibrations, the carbonate-related vibrations also decreased in intensity. We suggest that diffusion of protons within HT crystallites towards the interlayer leads to an equilibrium with the protonated anions in the interlayer, which is controlled by the acid–base reactions of the interlayer anions [Eqs. (1) and (2)].

$$CO_3^{2-} + H^+_{cationlayer} \rightarrow HCO_3^- \quad (1)$$

$$C_2O_4^{2-} + H^+_{cationlayer} \rightarrow HC_2O_4^- \quad (2)$$

This can explain why the thermal stability of HT_{ox} is higher than that of HT-CO_3, since the acid–base equilibrium of the oxalate ions is situated more on the nonprotonated side. Proton transfer will induce further dehydroxylation, since the resulting cation layer structure is unstable, as indicated by the higher percentages of tetrahedrally coordinated Al in HT-CO_3 at 473 K and 523 K than those in HT_{ox} at 523 K. This could explain the observed change in symmetry of interlayer carbonate and the appearance of the FT-IR signal at 1517 cm^{-1} for the HT-CO_3, which can now be related to bicarbonate formation.

TEM and XRD of heat-treated HTs: In general, XRD patterns of HTs calcined up to 773 K consist of broadened peaks that can be assigned to the corresponding metal oxides. Calcination of Mg–Al HTs results in the formation of an MgO-like phase. It has been proposed that the trivalent metal ions, in this case Al^{3+}, segregate from the decomposing cation layer and take part in the formation of spinel nuclei, which are not apparent in XRD analysis because of poor crystallinity and/or small crystallite sizes. In the literature several different spinel structures have been proposed, depending on the composition of the HT-like compound (the nature of the di- and trivalent cations and interlayer anions).[48, 56] Bright-field TEM images of calcined HTs show that the size and the shape of the original platelets after synthesis are maintained upon heating,[28] leaving only the possibility of small crystalline MgO-like domains. One way to confirm this proposition is the application of dark-field TEM. With this technique the incident electron beam is tilted, causing only diffracted electrons to be detected that have interacted more strongly with the sample. Thus unique structural information can be gathered.

The bright-field TEM image (Figure 8a) of an HT-CO_3 hydrothermally aged at 423 K after calcination at 723 K ($HT423_{calcinate}$) shows that heat treatment resulted in a roughening of the platelet basal surface, whereas the platelet size

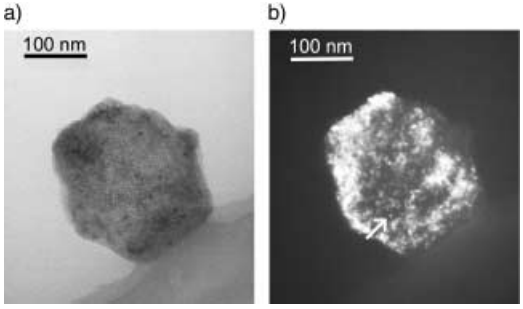

Figure 8. TEM images of $HT423_{calcinate}$: a) bright-field and b) dark-field (arrow indicates an Mg(Al)O domain of about 5 nm).

and shape had been retained, similarly to results of Reichle et al.[28] XRD reveals that the layered structure of HT had disappeared, as can be concluded from the absence of the (00*l*) reflections in Figure 9 when compared with the XRD pattern shown in Figure 2a. The broadened reflections that

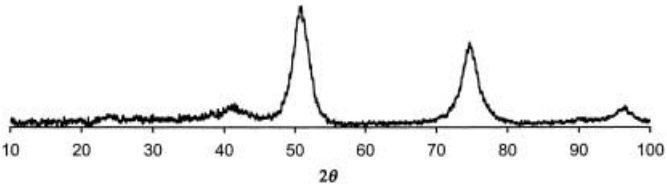

Figure 9. XRD pattern of $HT423_{calcinate}$.

appear have been indexed and compared with the *hkl* reflections of pure MgO (PDF file 45-0946; see Table 2). The lattice constant *a* was calculated from the (200) reflection to be 0.418 nm, by means of the expression for d_{hkl} spacings for the cubic crystal system,[49] which is similar to the value (0.417 nm) for a HT calcined at 773 K as reported by Hibino et al.[25] Presumably, the absence of the (311) reflection is caused by the intensity of the broadened signals being too low. Most measured *d* values included in Table 2 are slightly lower than those of pure MgO (2.43 Å), except for the (111) reflection, which is considerably higher (2.52 Å) and more intense. Kloprogge et al. ascribed this reflection without further exemplification to the (311) reflection of

Table 2. MgO diffraction data.

hkl	Intensity [%][a]	*d* [Å][a]	2Θ [°][a]	XRD Intensity [%]	*d* [Å]	TEM *d* [Å][b]
111	4	2.43	41.3	16	2.52	2.57 (s)
200	100	2.11	50.9	100	2.07	2.09 (r)
220	39	1.49	74.7	68	1.47	1.48 (s)
311	5	1.27	n.o.[c]	n.o.[c]	n.o.[c]	n.o.[c]
222	10	1.22	96.6	14	1.20	1.19 (r)
422	14	0.86	n.o.[d]	n.o.[d]	n.o.[d]	0.86 (s)

[a] Reference file PDF 45–0946; [b] s = spot, r = ring in Figure 10; [c] not observed; [d] beyond detection limit.

0947-6539/02/0824-5576 $ 20.00+.50/0 *Chem. Eur. J.* **2002**, *8*, No. 24

$MgAl_2O_4$.[50, 51] However, the spinel (311) reflection is found at 2.44 Å. XRD results of HT calcined at different temperatures by Aramendia et al. showed two distinct signals from the (311) spinel reflection and the (111) reflection of MgO at 1073 K.[52] Rebours et al. ascribed the reflection at 2.53 Å to the presence of cations on tetrahedral sites, possibly as a disordered spinel-type phase causing the broadening of this reflection.[24]

The electron diffraction patterns of HT with interlayer carbonate after synthesis at 423 K ($HT423_{as}$) and after calcination at 723 K ($HT423_{calcinate}$) are identical (Figure 10), showing that $HT423_{as}$ must have decomposed instantly in the

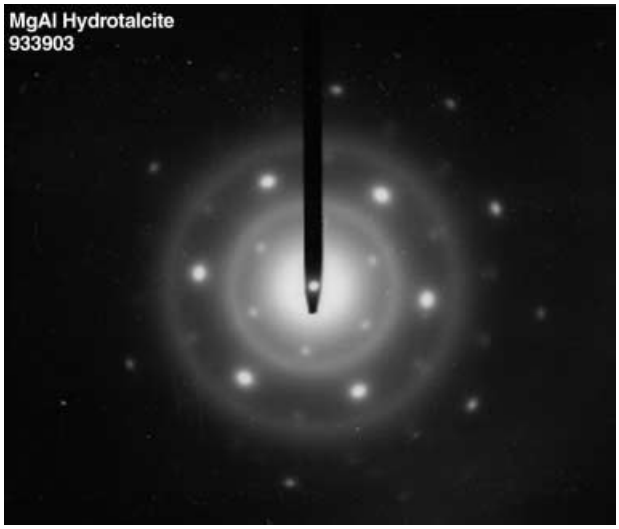

Figure 10. TEM diffraction pattern of $HT423_{calcinate}$.

intense electron beam during collection of the diffraction pattern. Lopez-Salinas et al. reported that Mg – Ga HT-like compounds are stable under the conditions applied in HR TEM. However, many structural defects were found that could have been brought about by the intense electron beam during the investigation.[53] The corresponding *d* values obtained from Figure 10 were, within the error of the measurement, identical to those obtained from XRD analysis. Again, most *d* values were slightly lower, which is attributable to the presence of Al^{3+} in the rock salt structure (Table 2). The electron diffraction pattern can only be caused by crystalline material. Due to the short wavelength of the electrons (< 0.1 nm) broadening of the reflections is much less than with X-rays (wavelength ≈ 0.3 nm). Several authors have ascribed the broadening of peaks in XRD to poorly crystalline MgO.[24, 54, 55] Our results clearly indicate the presence of small crystalline MgO domains. Decisive results from bright- and dark-field TEM originating from the same sample area (Figure 8a,b) show very small crystalline MgO domains within the heat-treated HT crystallite. The average crystallite size calculated from the (200) reflection from Figure 9 was 4.6 nm, which is in close agreement with the recent results from Sanchez et al. Using the same procedure, they found an average crystal size of 3.8 nm for an Mg – Al HT synthesized at 338 K and heat-treated at 723 K.[54] From Figure 8b we determined the length of an isolated domain (as indicated by the arrow), which was also about 5 nm. If we assume that this length represents the average size of an MgO-like domain, we can conclude that these small domains within the crystallites cause the broadened XRD pattern, as suggested by MacKenzie et al.[17]

Removal of interlayer water and dehydroxylation of the brucite-like layers, induced by proton diffusion, resulted in the observed decrease of the interlayer distance from 3.0 to 2.3 Å for the $HT\text{-}CO_3$ at 523 K (Figure 2a). This causes the formation of an Mg(Al)O phase in a direction parallel to the original interlayer. Disordered bonds, caused by nonideal packing, are probably then formed between two consecutive layers. Consequently the *d* value of the (111) reflection of the resulting MgO-like phase after heat treatment at 773 K is increased from the normal 2.44 Å to the 2.52 – 2.57 Å observed in XRD and in the TEM diffraction mode, which is not consistent with the other observed *d* values of the MgO-like phase (Table 2). The occurrence of spots in Figure 10 suggests that small Mg(Al)O crystallites are aligned, possibly parallel to the basal plane of the original HT structure. The rings in Figure 10, however, indicate random orientation in other directions. The partial orientation of the Mg(Al)O domains may be crucial for the so-called "memory effect" of HT, that is, the facile reconstruction of the layered HT structure after exposure of the calcined material to water.[7–13]

Conclusion

The results obtained with the various techniques all show the same general trend: the thermal behaviour of HT_{ox} is different from that of $HT\text{-}CO_3$. TGA-MS results demonstrate that the HT_{ox} contains only a small amount of interlayer water at room temperature. HT_{ox} exhibits only a small increase in tetrahedrally coordinated Al during heating to 473 K (Table 1). A decrease in the interlayer space was not observed in XRD up to 523 K and no substantial water release was detected up to 473 K, in contrast to what we observed with $HT\text{-}CO_3$. It has been proposed that dehydroxylation first proceeds within one layer, and that only after removal of carboxyl ions does dehydroxylation between two consecutive layers occur.[18] This last process is accompanied by loss of the lamellar arrangement of the layers, which brings about the drastic changes in the XRD pattern.

The nature of the interlayer anion greatly affects the onset of the dehydroxylation. Basic anions (carbonate, hydroxyl) abstract the protons from the hydroxyl ions in the layers more easily than the weakly basic oxalate. Until now, the removal of interlayer water was thought to instigate the dehydroxylation of HT compounds.[23, 56] However, our results show that the basicity of the interlayer anion is the crucial factor. In this way, dehydroxylation can be postponed beyond 473 K. Even at 523 K, still only 10% of the Al of HT_{ox} is tetrahedrally coordinated. Small Mg(Al)O domains (≈ 5 nm) within the thermally treated HT crystallites cause broadening of the XRD reflections. The diffraction pattern from TEM consists of spots and rings, caused by partly oriented crystalline material. Formation of disordered bonds, caused by nonideal packing, between the decomposing adjacent cation layers in

  0947-6539/02/0824-5577 $ 20.00+.50/0

the (1 1 1) direction could explain the increased *d* value of this reflection in the resulting MgO-like phase, observed with XRD and TEM in diffraction mode. The orientation of the small Mg(Al)O domains may be crucial for the so-called "memory effect" of HTs.

Experimental

Sample preparation: An aqueous solution (45 mL) of $Mg(NO_3)_2 \cdot 6H_2O$ (0.1 mol) and $Al(NO_3)_3 \cdot 9H_2O$ (0.05 mol) was added all at once to a second solution (70 mL) containing NaOH (0.35 mol) and Na_2CO_3 (0.09 mol) at 333 K. The resulting mixture was kept at this temperature for 24 h under vigorous stirring, after which the white precipitate was filtered off and washed several times. The HT was dried for 24 h at 393 K. This procedure resulted in the as-synthesized sample, designated HT-CO_3. ICP analysis revealed an Mg/Al ratio of 2.2:1.

The HT with oxalate as compensating anion (HT_{ox}) was synthesized by using the Titulaer procedure.[57] An aqueous solution (25 mL) of $MgCl_2 \cdot 6H_2O$ (0.04 mol) and $AlCl_3 \cdot 6H_2O$ (0.02 mol) was added all at once to a second solution (66 mL) containing $C_2H_2O_4 \cdot 2H_2O$ (6.3 mmol) and KOH (0.13 mol) under a nitrogen atmosphere. All solutions had been previously boiled and outgassed to remove carbon dioxide. The suspension was stirred at 293 K for 90 min, after which a third solution (66 mL) containing $C_2H_2O_4 \cdot 2H_2O$ (0.02 mol) and KOH (0.04 mol) was added. The resulting suspension was stirred at 367 K for 20 h. The white precipitate was filtered off and washed several times. The HT_{ox} was dried for 24 h at 333 K under a nitrogen atmosphere. ICP analysis revealed an Mg/Al ratio of 2.2:1.

To increase the crystallite size of the HT sample used in the TEM study, the HT was synthesized under hydrothermal conditions, similar to those of Reichle et al.[28]

An aqueous solution (45 mL) of $Mg(NO_3)_2 \cdot 6H_2O$ (0.1 mol) and $Al(NO_3)_3 \cdot 9H_2O$ (0.05 mol) was added all at once to a second solution (70 mL) containing NaOH (0.35 mol) and Na_2CO_3 (0.09 mol) at 333 K. The mixture was kept at this temperature for 1 h under stirring, then the suspension with the white precipitate was poured into a Teflon holder and placed in a stainless-steel rotating autoclave. After a 24 h crystallization and ageing period at 423 K, the white precipitate was filtered and washed several times. The HT was dried for 24 h at 393 K. This procedure resulted in the as-synthesized sample designated as $HT423_{as}$. After drying, the HT was heated at 10 K min^{-1} in a nitrogen flow to 723 K and kept at that temperature for 8 h. The sample after heat treatment ($HT423_{calcinate}$) was stored under a nitrogen atmosphere. ICP analysis revealed an Mg/Al ratio of 2.3:1.

Transmission electron microscopy: TEM images were obtained with a Philips EM-420 transmission electron microscope operated at 120 kV. After ultrasonic treatment in ethanol, samples were dispersed on a holey carbon film. A gold standard film was used to calibrate the electron microscope diffraction parameters.

X-ray diffraction: XRD patterns were measured by using an Enraf–Nonius CPS 120 powder diffraction apparatus with $Co_{K\alpha}$ radiation ($\lambda =$ 1.78897 Å). Before measurement, ex situ samples were heated at 5 K min^{-1} under a nitrogen atmosphere to the desired temperature, which was then maintained for 1 h; the sample was subsequently cooled to room temperature and stored under nitrogen. Measurements were performed in air at room temperature. In situ high-temperature measurements were performed in a high-temperature cell (Anton Paar) under a controlled atmosphere: a constant flow of nitrogen was used to avoid exposure of the samples to atmospheric carbon dioxide and water. A heating rate of 10 K min^{-1} was applied and diffraction patterns were measured for 1 h at the desired temperature (room temperature, 423 K and 473 K), which was kept constant during measurement.

XANES measurements: XANES measurements were performed at beamline 3.4 at the SRS, Daresbury (UK). The in situ low-energy X-ray absorption fine structure (ILEXAFS) set-up had been developed for in situ XAFS measurements in the range 1000–3500 eV. Measurements could be performed in a gaseous environment (with a maximum pressure of 1 bar) at temperatures from 80 to 750 K.[58] Both electron yield (measuring drain current) and fluorescence yield (using a gas proportional counter) were detected; they gave very similar results. For the XANES analyses, fluorescence spectra were pre-edged, background subtracted and normalized.

The samples were heated to 373 K at 10 K min^{-1} and then to 523 K at 0.5 K min^{-1} and measured at temperature intervals of 10 K in situ at the Al K-edge. K-edges were measured in situ at room temperature, 423 K, 473 K and 523 K.

^{27}Al MAS-NMR: ^{27}Al MAS-NMR experiments were carried out on a Chemagnetics Infinity 600 apparatus (14.1 T) operating at 156.3 MHz. Samples were loaded in a Chemagnetics 2.5 mm HX MAS probe, making possible magic-angle spinning at a rotation speed of 25–27 kHz. To allow quantitative evaluation of the single-pulse excitation (SPE) spectra, $\pi/18$ pulses using an RF field strength of approximately 40 kHz were used. Chemical shifts were referenced relative to an aqueous $Al(NO_3)_3$ solution. The relaxation delays were 10 s, determined to be adequate for quantitative analyses using saturation recovery experiments. The peak intensities were integrated with the help of a program developed in MATLAB.

Before measurement, samples were heated at 5 K min^{-1} under a nitrogen atmosphere. The desired temperature was maintained for 1 h and the sample was subsequently cooled to room temperature and stored under nitrogen. Spectra were obtained at room temperature in air from samples pretreated at room temperature, 423 K, 473 K and 523 K.

Infrared spectroscopy: IR spectra were recorded with an FT-IR Perkin-Elmer 1720-X spectrometer by using KBr windows and the KBr pellet technique. Spectra were obtained under a helium flow with a resolution of 4 cm^{-1} at room temperature, 423 K, 473 K and 523 K; the heating rate was 5 K min^{-1}. The Perkin–Elmer Spectrum V3.01 program was used for data analysis.

TGA: TGA analyses were carried out on a Netzsch STA-429 thermobalance. The gases evolved during analysis were monitored by a Fisons Thermolab quadrupole mass spectrometer, with a capillary situated directly above the sample cup. Samples were heated in nitrogen at 10 K min^{-1}.

Acknowledgement

We thank Ad van der Eerden and Andy Smith for their help with the XANES experiments and Michiel Oudenhuijzen and Harry Bitter for the FT-IR measurements. Financial support from the Innovation Oriented Research Programmes (IOP), an initiative of the Dutch Ministry of Economic Affairs, is gratefully acknowledged.

[1] J. I. Di Cosimo, V. K. Diez, M. Xu, E. Iglesia, C. R. Apesteguia, *J. Catal.* **1998**, *178*, 499.
[2] W. T. Reichle, *J. Catal.* **1980**, *63*, 295.
[3] E. Suzuki, Y. Ono, *Bull. Chem. Soc. Jpn.* **1988**, *61*, 1008.
[4] A. Corma, R. Martin-Aranda, *Appl. Catal.* **1993**, *105*, 271.
[5] M. J. Climent, A. Corma, S. Iborra, J. Primo, *J. Catal.* **1995**, *151*, 60.
[6] V. R. L. Constantino, T. J. Pinnavaia, *Catal. Lett.* **1994**, *23*, 361.
[7] S. Miyata, *Clays Clay Miner.* **1980**, *28*, 50.
[8] D. Tichit, M. Naciri Bennani, F. Figueras, R. Teissier, J. Kervenal, *Appl. Clay. Sci.* **1998**, *13*, 401.
[9] F. Prinetto, D. Tichit, R. Teissier, B. Coq, *Catal. Today* **2000**, *55*, 103.
[10] J. C. A. A. Roelofs, A. J. van Dillen, K. P. de Jong, *Catal. Today* **2000**, *60*, 297.
[11] K. Koteswara Rao, M. Gravelle, J. Valente, F. Figueras, *J. Catal.* **1998**, *173*, 115.
[12] J. C. A. A. Roelofs, A. J. van Dillen, K. P. de Jong, *Catal. Lett.* **2001**, *74*, 91.
[13] F. Cavani., F. Trifiro, A. Vaccari, *Catal. Today* **1991**, *11*, 173.
[14] A. van dern Pol, B. L. Mojet, E. van dern Ven, E. de Boer, *J. Phys. Chem. B* **1994**, *98*, 4050.
[15] W. Kagunya, P. Dutta, Z. Lei, *Physica B* **1997**, *234*, 910.
[16] M. J. Hudson, S. Carlino, D. C. Apperley, *J. Mater. Chem.* **1995**, *5*, 323.
[17] K. J. D. MacKenzie, R. H. Meinhold, B. L. Sherriff, Z. Xu, *J. Mater. Chem.* **1993**, *3*, 1263.

  0947-6539/02/0824-5578 $ 20.00+.50/0 *Chem. Eur. J.* **2002**, *8*, No. 24

[18] F. Rey, V. Fornes, J. M. Rojo, *J. Chem. Soc. Faraday Trans.* **1992**, *88*, 2233.
[19] J. Rocha, M. del Arco, V. Rives, M. A. Ulibarri, *J. Mater. Chem.* **1999**, *9*, 2499.
[20] V. Rives, *Inorg. Chem.* **1999**, *38*, 406.
[21] Z. P. Xu, H. C. Peng, *Chem. Mater*. **2001**, *13*, 4564.
[22] O. Clause, B. Rebours, E. Merlen, F. Trifiro, A. Vaccari, *J. Catal.* **1992**, *133*, 231.
[23] M. Belotto, B. Rebours, O. Clause, J. Lynch, *J. Phys. Chem. B* **1996**, *100*, 8535.
[24] B. Rebours, J.-P. D'Espinose de la Caillerie, O. Clause, *J. Am. Chem. Soc.* **1994**, *116*, 1707.
[25] T. Hibino, Y. Yamashita, K. Kosuge, A. Tsunashima, *Clays. Clay. Miner.* **1995**, *43*, 427.
[26] E. Kanezaki, *Inorg. Chem.* **1998**, *37*, 2588.
[27] T. Hibino, A. Tsunashima, *Chem. Mater.* **1998**, *10*, 4055.
[28] W. T. Reichle, S. Kang, D. S. Everhardt, *J. Catal.* **1986**, *101*, 352.
[29] J. C. A. A. Roelofs, D. J. Lensveld, A. J. Van Dillen, K. P. De Jong, *J. Catal.* **2001**, *203*, 184.
[30] M. A. Ulibarri, I. Pavlovic, C. Barriga, M. C. Hermosin, J.Cornejo, *Appl. Clay. Sci.* **2001**, *18*, 17.
[31] J. A. Van Bokhoven, J. C. A. A. Roelofs, K. P. de Jong, D. C. Koningsberger, *Chem. Eur. J.* **2001**, *7*, 1258.
[32] M. A. Drezdon, *Inorg. Chem.* **1988**, *37*, 4628.
[33] S. Miyata, T. Kumura, *Chem. Lett.* **1973**, 843.
[34] M. Vucelic, G. D. Moggridge, W. Jones, *J. Phys. Chem. B* **1995**, *99*, 8328.
[35] M. C. Gastuche, G. Brown, M. M. Mortland, *Clay Miner.* **1967**, *7*, 177.
[36] C. J. Serna, J. L. Rendon, J. E. Iglesias, *Clays Clay Miner.* **1982**, *30*, 180.
[37] D. Tichit, M. N. Bennani, F. Figueras, J. R. Ruiz, *Langmuir* **1998**, *14*, 2086.
[38] V. R. L. Constantino, T. J. Pinnavaia, *Inorg. Chem.* **1995**, *34*, 883.
[39] F. Malherbe, J. P. Besse, *J.Solid State Chem.* **2000**, *155*, 332.
[40] H. Kraus, R. Prins, A. P. M. Kentgens, *J. Phys. Chem. B* **1996**, *100*, 16336.
[41] A. P. M. Kentgens, *Geoderma* **1997**, *80*, 271.
[42] T. Yoshida, T. Tanaka, H. Yoshida, S. Takenaka, T. Funabiki, S. Yoshida, T. Murata, *Physica B* **1995**, *208*, 581.
[43] J. T. Kloprogge, R. L. Frost, *J. Solid State Chem.* **1999**, *146*, 506.
[44] M. J. Hernandez-Moreno, M. A. Ulibarri, J. L. Rendon, C. J. Serna, *Phys. Chem. Miner.* **1985**, *12*, 34.
[45] S. Miyata, *Clays Clay Miner.* **1974**, *23*, 369.
[46] V. Prevot, C. Forano, J. P. Besse, *Appl. Clay Sci.* **2001**, *18*, 3.
[47] T. S. Stanimirova, I. Vergilov, G. Kirov, N. Petrova, *J. Mater. Sci.* **1999**, *34*, 3153.
[48] T. Hibino, A. Tsunashima, *J. Mater. Sci. Lett.* **2000**, *19*, 1403.
[49] M. T. Weller, *Inorganic Materials Chemistry*, Oxford University Press, London, **1996**.
[50] J. T. Kloprogge, R. L. Frost, *Appl. Catal. A*. **1999**, *184*, 61.
[51] J. T. Kloprogge, L. Hickey, R. L. Frost, *Appl. Clay. Sci.* **2001**, *18*, 37.
[52] M. A. Aramendia, Y. Aviles, V. Borau, J. M. Luque, J. M. Marinas, J. A. Ruiz, F. J. Urbano, *J. Mater. Chem.* **1999**, *9*, 1603.
[53] E. Lopez-Salinas, M. Garcia-Sanchez, J. A. Montoya, D. R. Acosta, J. A. Abasolo, I. Schifter, *Langmuir* **1997**, *13*, 4748.
[54] J. Sanchez Valente, F. Figueras, M. Gravelle, P. Kumbnar, J. Lopez, J. P. Besse, *J. Catal.* **2001**, *189*, 370.
[55] J. M. Fernandez, M. A. Ulibarri, F. M. Labajos, V. Rives, *J. Mater. Chem.* **1998**, *8*, 2507.
[56] J. Perez-Ramirez, G. Mul, F. Kapteijn, J. A. Moulijn, *J. Mater. Chem.* **2001**, *11*, 821.
[57] M. K. Titulaer, Ph.D thesis, Utrecht University, **1993**.
[58] J. A. Van Bokhoven, A. M. J. Van der Eerden, A. D. Smith, D. C. Koningsberger, *J. Synchrotron Radiat.* **1999**, *6*, 201.

Received: June 10, 2002 [F4168]